

## Emitter Wrap Through Solar Cells using Electroless Plating Metallisation

H. Knauss, W. Jooss, S. Roberts\*, T.M. Bruton\*, R. Toelle\*, P. Fath, E. Bucher,  
*University of Konstanz, Department of Physics, P.O.Box X916, D-78457 Konstanz, Germany*  
 Phone: +49-7531-88-2082, Fax: +49-7531-88-3895  
 Author for correspondence: Holger Knauss, e-mail: [Holger.Knauss@uni-konstanz.de](mailto:Holger.Knauss@uni-konstanz.de)  
 \*BP Solar, 12 Brooklands Close, Windmill Road, Sunbury-on-Thames, Mddx TW16 7DX, United Kingdom

**ABSTRACT:** Back contact solar cells are considered as the possible next generation crystalline silicon solar cells. They offer the advantages of reduced shading losses, a much easier module assembly and additional charge carrier collection by the emitter on the rear side. With Emitter Wrap Through (EWT) solar cells the front side emitter is connected to the n-type contact on the rear side via small laser drilled holes. In this paper we present a realisation of an Emitter Wrap Through solar cell using electroless plating metallisation. The suggested process uses only technologies applicable to industrial production and avoids photolithography. The best EWT cells reached efficiencies up to 16.6% (23 cm<sup>2</sup>, Cz-Si). To allow a more detailed analysis of the EWT cells two types of reference cells were processed in parallel. The characterisation of all three types of cells led to the conclusion that recombination caused by an incompletely removed laser damage currently limits the performance of our EWT cells.

**Keywords:** Emitter Wrap Through – 1: Buried Contact – 2: Back contact – 3:

### 1. INTRODUCTION

Back contact solar cells offer various advantages over conventionally designed solar cells. Previous investigations showed that module assembly costs could be significantly reduced due to the back contact design [1]. Furthermore by placing the metal contact on the rear of the solar cell, the active front surface area can be increased due to lower shading losses. Recently several device designs have been suggested and investigated including the Emitter Wrap Through (EWT) solar cell [2]. In this device the metal contacts of both polarities are located on the rear side. The n-type contact on the rear side is connected to the front side emitter through laser drilled holes (see Fig. 1). With collecting junctions on both sides of the cell the concept is considered particularly suited for material with low bulk diffusion lengths.

Most low cost realisations of this cell type used thick film technology for metallisation. This approach led to efficiencies up to 16.1% [3]. Screen printed cells suffered so far from a high series resistance.

Very little effort has been done for the processing of

EWT solar cells applying the technique of electroless plating as it is used for Buried Contact Solar Cells (BCSC)[4], [5]. In our labs this technology has already been successfully transferred to the production of MWA and MWT back contact cells [6]. Up to this point only moderate efficiencies ( $\eta=8.8\%$ ) were reached for EWT cells despite the fact that the formation of the metal contacts by electroless plating offers several advantages: The self aligning character of the technology removes one alignment step and results in a reliable metallisation of the vias. Increasing the thickness of the deposited copper layer compared to conventional BC cells allows low series resistances.

Furthermore the use of the electroless plating metallisation allows an easy realisation of different cell designs. This fact was taken advantage of by processing two types of reference cells, so that a more detailed characterisation of the loss mechanisms limiting our EWT cell performance is possible.

### 2. CELL PROCESSING

The design of the Emitter Wrap Through solar cell in this work includes a selective emitter, which means a lightly doped emitter on the front side and a heavily doped emitter underneath the contacts. n-type regions on the rear are only underneath the n-type finger contact (about 15% of the rear side), whereas the other parts are either passivated by silicon nitride (non contacted area) or an Al-BSF (area underneath the p-type contact). The p- and n-type contact fingers are formed by laser scribing, which is done in parallel with the hole formation.

The applied processing sequence is very similar to the one of conventional BCSCs (see Fig.2). Processing of the EWT solar cell starts with alkaline texturing which is followed by a  $\text{POCl}_3$  emitter diffusion ( $R_{\text{sheet}} \approx 80-100 \Omega/\text{sq}$ ). The next step is the deposition of silicon nitride by Low Pressure CVD on the front side (wafers are

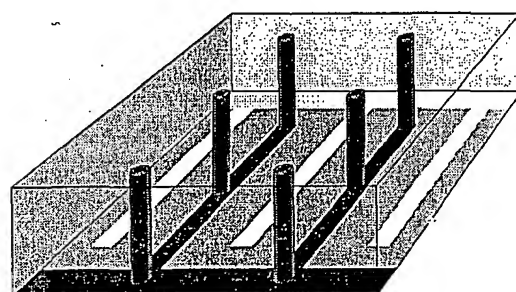


Figure1: Schematic illustration of an EWT solar cell. Two interdigitated contact grids are located on the rear side. The n-type contact (dark) is connected to the emitter on the front side via holes.

back-to-back during deposition). The rear side emitter was removed in a hot solution of NaOH, then  $\text{SiN}_x$  is deposited on the rear side. In principle, a much simpler manufacturing sequence is possible if processing starts with a single side diffusion, which is followed by the deposition of  $\text{SiN}_x$  in an LPCVD-system on front and rear.

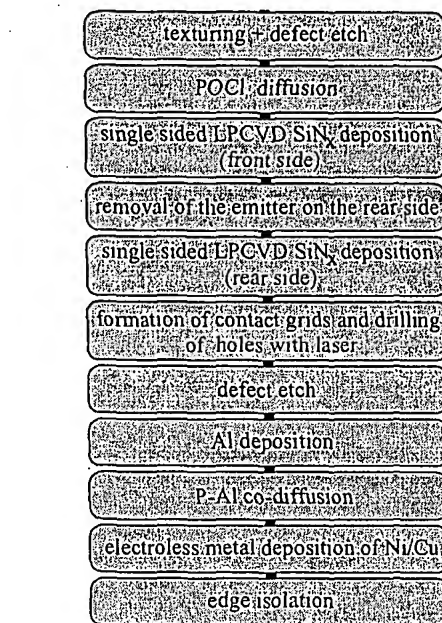


Figure 2: Applied process sequence for EWT solar cells using electroless metallisation.

In the applied process the nitride serves for surface passivation, anti reflection coating and most important, as a mask during electroless plating. In the next step, the holes are drilled and the buried contacts of the n and p-type fingers and busbars are formed by laser ablation. The laser damage is removed in a hot solution of NaOH. A very important step in our processing sequence is P-Al co-diffusion: Al is evaporated on the regions of the p-type contact grooves (other regions are protected by shadowing masks) before the co-diffusion. This allows a simplification of the process in two aspects: First one high temperature step is avoided; second masking which would be necessary otherwise can be eliminated (compare e.g. [2]). During the co-diffusion the vias and n-type contact areas obtain a heavy P-diffusion ( $R_{sheet} = 10 \Omega/\text{sq}$ ), whereas in the p-type grooves the Al-BSF is formed. Metallisation is done by electroless deposition of Ni/Cu. During the electroless plating step the p- and n-type grooves on the rear as well as the holes get metallised. The deposition of the EWT cell was increased compared to the reference cells, which allowed a reduction in series resistance (approx.  $0.1 \Omega\text{cm}^2$  compared to normal deposition time). Processing is finished by edge isolation.

### 3. CELL CHARACTERISATION

In this study, two different types of reference cells were processed in parallel. The first one is a conventional buried

contact solar cell with a full area Al-BSF (Process A), the second one (Process B) has LPCVD- $\text{SiN}_x$  on its rear side, which is removed by laser ablation in areas where the local p-type contact is formed. The front contact grooves, which are identical for both reference cells, were cut with a dicing saw. The design of the local base contact in process B is identical to the base contact grid of the EWT cells. Again evaporation of Al was done before P-Al co-diffusion.

Solar cells were processed according to the described sequences using solar grade Cz-Si (initial wafer size  $12.5 \times 12.5 \text{ cm}^2$ ). From each wafer four cells were processed: two EWT solar cells, one conventional with full area BSF (Process A) and one solar cell with local BSF (Process B) each with a cell area of  $23 \text{ cm}^2$  after edge isolation. The illuminated I-V-parameters of the best cell of each type are listed in Tab. I.

Table I: Illuminated I-V-parameters of the best cell of each type.

	EWT	Process A	Process B
$\eta [\%]$	16.6	16.6	16.0
$V_{OC} [\text{mV}]$	591	612	607
$J_{SC} [\text{mV}]$	37.7	35.1	34.7
FF [%]	74.6	77.2	76.0

The saturation current densities  $J_{01}$  and  $J_{02}$  of the first and second diode were fitted to the  $J_{SC}$ - $V_{OC}$ -curve assuming ideality factors of  $n_1=1$  and  $n_2=2$ . The shunt resistance  $R_{shunt}$  was taken from the dark I-V-measurement, while the series resistance  $R_{series}$  was determined from the illuminated curve.

Table II: Fitted Parameters of the two-diode-model.

	EWT	Process A	Process B
$R_{shunt} [\Omega\text{cm}^2]$	1600	1900	1200
$R_{series} [\Omega\text{cm}^2]$	0.72	0.62	0.84
$J_{01} [10^{-12} \text{ A/cm}^2]$	2.5	1.3	1.5
$J_{02} [10^{-8} \text{ A/cm}^2]$	8.9	4.1	4.3

Comparing the illuminated I-V-parameters of the different types of solar cells shows on the one hand a significant increase in short circuit current density  $J_{SC}$  of the EWT cell, but on the other hand the open circuit voltage  $V_{OC}$  is reduced.

The increased  $J_{SC}$  of the EWT cell can mainly be attributed to the nearly non-existent shadowing loss of the front metallisation. Fig. 4 shows a LBIC scan, where the positive effect of double-sided minority carrier collection is visible. But since only about 15% of the rear side is covered with emitter, the beneficial influence can almost be neglected. However the EWT cell does have the best External Quantum Efficiency (EQE) in the long wavelength range ( $\lambda > 900 \text{ nm}$ ), but the increased EQE is also caused by different optical qualities of the rear sides (see Fig. 3). The reflectance measurement shows that the Al-BSF tends to absorb long wavelength light, while it is reflected at the surfaces passivated with LPCVD  $\text{SiN}_x$ . The difference in  $J_{SC}$  of Process A and Process B is caused

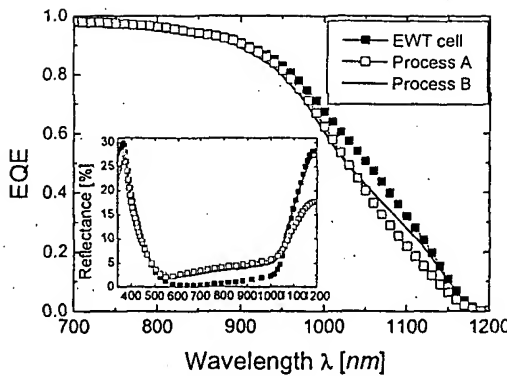


Figure 3: External Quantum Efficiency (EQE) and Reflectance Measurement. BC EWT cell: solid squares; conventional BC cell: hollow squares; conventional BC cell with local back contact: no symbol

by the different rear side passivation. The passivation by LPCVD-SiN<sub>x</sub> (Process B) is not as good as for the Al-BSF (Process A), which can be seen in Fig. 5. Here the areas passivated with Al-BSF clearly show an increased current. The EWT cell shows the best EQE in the long wavelength range. This is a benefit of double-sided charge carrier collection as well as of the optical properties of its rear side.

Different passivation of the rear side is also the reason for the lower value of  $J_{01}$  of Process A compared to Process B. As a consequence a drop in  $V_{OC}$  can be observed.  $V_{OC}$  of the EWT cell is even smaller. A decrease in the open circuit voltage of EWT cells was noticed for several realisations using low cost technologies. As [7] showed this decrease is a consequence of the different cell geometry. If the diffusion length is lower than about half the thickness of the wafer, additional carrier injection at the emitter on the rear side increases  $J_{01}$ . However since only about 15% of the rear side is covered with emitter, the one-dimensional model cannot explain a drop in  $V_{OC}$  of the magnitude observed. LBIC scans [8] did not show any degradation of the minority charge carrier diffusion length in the silicon used for EWT cells compared to the reference cells. It is very likely that an incompletely removed laser damage causes additional recombination. This assumption was confirmed by a first investigation, where conventional BC cells with a laser grooved front contact were processed in our lab, which also showed an increased  $J_{01}$  compared to cells with a mechanically cut contact.

The laser damage might also be the reason for the increased saturation current of the second diode  $J_{02}$ . Again the different cell geometry raises  $J_{02}$ , but cannot fully explain the increase observed.

Despite the relatively high  $J_{02}$  the fill factor is remarkably good for EWT cells produced with industrial applicable technologies. This is due to the low series resistance which is nearly half the one measured for screen printed EWT cells [3].

Overall our cells obtained an efficiency of 16.6%, which is to our knowledge, the highest reported so far for an EWT cell produced with low cost technologies (without photolithography). The efficiency is as high as that of the

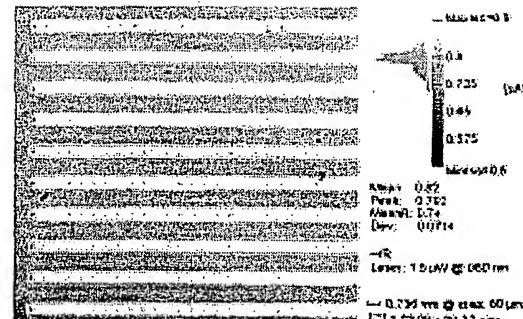


Figure 4: LBIC scan of a part of an EWT cell (wavelength 980nm). The emitter under the n-type contact collects minority charge carriers on the rear side. This additional collection increases the current, so that the region under the n-type contacts is much brighter than areas between them, where carriers are collected at the front surface only.

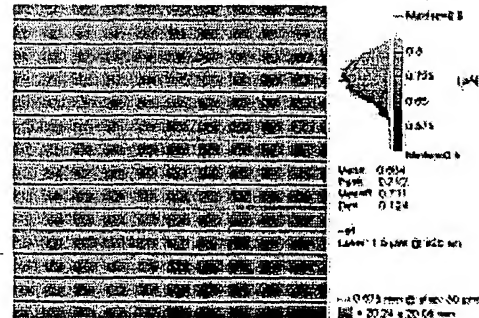


Figure 5: LBIC scan of a reference cell of Process B (wavelength 980nm). The passivation of LPCVD nitride is not as good as the one of an Al-BSF, which leads to the horizontal variation of the collected current. Close to the front fingers the collected current is also raised. This is due to additional collection of the vertical emitter in the contact grooves.

conventional BC reference cell. It is achieved by an increased short circuit current density  $J_{SC}$ , which compensates the drop in open circuit voltage.

If laser damage can be reduced either by increasing etching or optimising laser parameters, both the saturation current of the first as well as of the second diode should be remarkably lowered. Open circuit voltages over 605 mV and fill factors well above 75% should be easy to realize. In this case the overall efficiency would rise above 17.3%. Optimising the LPCVD nitride for a better passivation of the rear side promises further progress.

#### 4. CONCLUSIONS

EWT solar cells were produced using electroless plating metallisation technology, which seems to be especially suited for this cell concept. Cells with efficiencies up to 16.6% (24 cm<sup>2</sup>, Cz-Si) were produced, which is one of the

highest efficiencies reached with this cell design without photolithography. The series resistance of the cell was strongly reduced compared to EWT cells using thick film metallisation. The cell performance was limited by the saturation current densities  $J_{01}$  and  $J_{02}$ , which are likely to be caused by the incomplete removal of laser damage. With optimised laser parameters and the complete removal of laser damage, it should be possible to achieve efficiencies above 17.3% in the near future.

#### ACKNOWLEDGEMENTS

We would like to thank M. Keil for technical assistance during solar cell processing, T. Pernau for the LBIC-scans and B. Fischer for fruitful discussions. This work was supported within the JOULE project by the European Commission under contract number JOR-CT98-0269 (ACE Designs).

#### REFERENCES

- [1] J.M. Gee, S.E. Garrett, W.P. Morgan, "Simplified module assembly using back-contact crystalline-silicon solar cells", 26<sup>th</sup> IEEE PVSC, pp. 1085-88 (1997)
- [2] J.M. Gee, W. K. Schubert, P.A. Basore, "Emitter Wrap-Trough Solar Cell", Proc. 23<sup>rd</sup> IEEE PVSC, pp. 265-70 (1993)
- [3] A. Kress, R. Tölle, T. Bruton, P. Fath, E. Bucher, "10 x 10 cm<sup>2</sup> Screen printed back contact solar cell with a selective emitter", 28<sup>th</sup> IEEE PVSC, pp. 213-16 (2000)
- [4] C.B. Honsberg, F. Yun, M.A. Green, S.R. Wenham, "Mechanically grooved, multi-junction, interdigitated rear contact silicon solar cells for low cost substrates", 12<sup>th</sup> EC PVSEC, pp. 63-6 (1994)
- [5] J.M. Gee, M.E. Buck, W.K. Schubert, P.A. Basore, "Progress on the Emitter Wrap-Trough silicon solar cell", 12<sup>th</sup> EC PVSEC, pp. 743-46 (1994)
- [6] W.Jooss, K. Blaschek, R.Toelle, T.M. Bruton, P. Fath, E. Bucher, "17% Back Contact Buried Contact Cells", 16<sup>th</sup> EC PVSEC, pp. 1124-7 (2000)
- [7] E. Van Kerschaver, C. Zechner, J. Dicker, "Double Sided Minority Carrier Collection in Silicon Solar Cells", Trans. on Electron Devices 47, pp. 711-16 (2000)
- [8] T. Pernau, M. Spiegel, P. Fath, E. Bucher, "High-speed and high accuracy IQE and  $L_{eff}$ -mapping -a tool for advanced quality control in the PV-industry", to be published in Proc. 17<sup>th</sup> EC PVSEC, (2001)